THE IMPORTANCE OF FFT AND BCS SPECTRUMS ANALYSIS FOR DIAGNOSIS AND PREDICTION OF ROLLING BEARING FAILURE

Dumitru-Cristinel NADABAICĂ[1], Valentin NEDEFF[1], Stanisław RADKOWSKI[2], Jędrzej MĄCZAK[2]

[1]"Vasile Alecsandri" University of Bacau, Department of Environmental Engineering and Mechanical Engineering, Calea Marasesti 156, Bacau, 600115, Romania
e-mail: nadabaica.dumitru@ub.ro
[2]Warsaw University of Technology, Institute of Vehicles, Narbutta 84, 02-524 Warsaw, Poland
e-mail: ras@simr.pw.edu.pl; jma@mechatronika.net.pl

Abstract

Dynamic equipments, in their vast majority, have rolling bearings in their components. Measurement and analysis of the values of rolling bearings vibration, on time, represent a safe and effective measure for identifying the state of wear of bearings, and to predict the evolution of their technical condition and of the entire equipment. This paper presents the detection of causes which lead to the damage of rolling bearing by using FFT (Fast Fourier Transformation) and BCS (Bearing Condition Signature) spectrums, by measuring its housing vibrations (self-aligning ball bearing, ZKL 1205K type) mounted in a test rig. The results presents the analysis mode of FFT and BCS spectrums in order to obtain beneficial information for the detection of that unbalance caused by loading, of the implemented defect on rolling bearing raceway and of bearing damage mode under the action of these causes.

Keywords: FFT spectrum, BCS spectrum, rolling bearings, diagnose, prediction.

1. INTRODUCTION

Rolling bearings are the most common and critical components of dynamic equipment. Many predictive maintenance programs use modern methods for monitoring of rolling bearing during the exploring operation, in order to detect failures and diagnosis of rolling bearing, but also to avoid the disuse of it and of equipment. The most common causes that lead to vibrations in rolling bearings are: improper design, incorrect mounting, misalignment, unbalance, improper choice of rolling bearing type, long duration of use, improper lubrication, use of equipments to other parameters than those for which they were designed and others [1, 6]. Therefore it is important that the rolling bearings to be measured and analyzed and, when necessary, any defects identified by vibration analysis to be corrected in a predictive maintenance program [2].

The diagnosis by using the envelope technique is the processing of vibration signal in order to identify defects of rolling bearings and to extract characteristic defect frequencies. By using this analysis it is possible both to identify the defects within rolling bearings and their location (outer raceway, inner raceway, rolling elements, cage) [3, 4, 6].

When the rolling bearings are damaged the characteristic defect frequencies can be observed in vibration spectrums. The occurrence of these frequencies in vibration spectrums depend the faulty component of rolling bearing [5, 7, 8]. Defects in rolling bearings can be identified by vibration analysis, if the spectral components with typical defect frequencies (and their harmonics) are detects.

The FFT spectrums are obtained by using envelope technique of the modulating signal. These spectrums give information on the various causes that lead to the deterioration of rolling bearings (unbalance, misalignment, mechanical looseness and others). The BCS spectrums are obtained by using the amplitude demodulation technique from the amplitude modulated signal. These spectrums give us information on the condition of rolling bearing [9]. The characteristic defect frequencies of rolling bearings can be analyzed both in the FFT and BCS spectrums.

There are five defect characteristic frequencies of rolling bearings which can occur in the FFT and BCS spectrums [8]: cage ball-pass frequency (F_c); outer-raceway ball-pass frequency (F_{BPI}); inner-raceway ball-pass frequency (F_{BPO}); rolling-element rotational frequency (F_{RE}); rolling-element ball-pass frequency ($F_{BPRE} = 2x\ F_{RE}$). These frequencies can be calculated as:

$$F_c = \frac{1}{2} F_s \left(1 - \frac{D_b \cos\theta}{D}\right) \tag{1}$$

$$F_{BPI} = \frac{N_b}{2} F_s \left(1 + \frac{D_b \cos\theta}{D}\right) \tag{2}$$

$$F_{BPO} = \frac{N_b}{2} F_s \left(1 - \frac{D_b \cos\theta}{D}\right) \tag{3}$$

$$F_{RE} = \frac{D}{2\,D_b} F_s \left(1 - \frac{D_b^2 \cos^2\theta}{D^2}\right) \tag{4}$$

where: F_s is the fundamental frequency (rotating speed) of the shaft; D_b – the diameter ball; θ – the

contact angle; D – the pitch diameter of the rolling bearing; N_b – the number of balls.

2. EXPERIMENTAL RESEARCH

2.1. Test rig description

This experimental research has proposed the analysis of FFT and BCS spectrums in order to diagnose and predict failure of rolling bearings. Thus, the test rig consisted of a base on which the electric motor-gearbox-coupling-shaft assembly was mounted, as can be seen in Fig. 1. The electric motor has a power of 0.25 kW and a rotating speed of 2760 rpm. Since the gearbox ratio is 2.8 the shaft speed used is 1000 rpm. The shaft is supported by two rolling bearings, ZKL 1205K type. These are self-aligning ball bearing with tapered bore (taper 1:12) which are mounted on the shaft by means of adapter sleeves. The measurements were performed in the horizontal, vertical and axial directions of the rolling bearing housing from left side of the test rig.

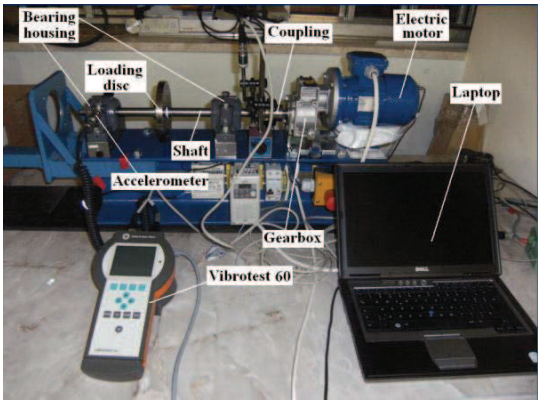

Fig. 1. Test rig

2.2. Vibration measuring devices

The acquisition of vibration measurements was performed by using a piezoelectric accelerometer (Fig. 2a) connected to the VIBROTEST 60 device (Fig. 2b) from Bruel & Kjaer Vibro. Measurements were recorded in the PC-card of VIBROTEST 60 device (Fig. 2c), then transferred for their analysis in the XMS software (**e**xtended **m**onitoring **s**oftware). The frequency range of the sensor is between 4 Hz and 10 kHz, and the resonance frequency is 35 kHz.

For the vibrations' analysis, an artificial defect was implemented on the outer raceway of the rolling bearing (Fig. 3), with its size given in Table 1. The rolling bearing worked under three loadings: 14 N, 24 N and 42 N (three steel discs of 1.4 kg each). The rolling bearing worked for 10 hours under each loading. The first measurement was acquired at the beginning of the experiment then another 5 measurements at intervals of two hours. Before each operation, between the second and third loading, the bearing was cleaned by using petrol and then it was re-lubricated. The vibration signals were collected in the frequency domain in order to analyze: overall vibration trend, overall BCU (Bearing Condition Unit) trend, FFT and BCS spectrum. The appearance and evolution mode of the characteristic defect frequencies' amplitude, their harmonics and the side bands of these frequencies and harmonics were analyzed in FFT and BCS spectrums.

a. b. c.

Fig. 2. Acquisition system of vibration from Bruel & Kjaer Vibro: a. – accelerometer, AS-065 type; b. – VIBROTEST 60 device; c. – PC-card

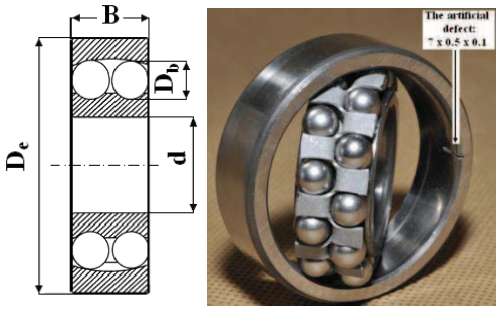

a. b.

Fig. 3. Self-aligning ball bearing with tapered bore, ZKL 1205K type: a. - technical drawing; b. - photo with location of the artificial defect on rolling bearing outer raceway

The geometrical characteristics of this type of bearing are shown in Table 2.

Table 1. Sizes of the artificial defect on rolling bearing outer raceway

Defect cod	Length [mm]	Width [mm]	Depth [mm]
D1E	7	0.5	0.1

Table 2. Sizes of self-aligning ball bearing with tapered bore, ZKL 1205K type

Sizes	Values
D_e - outer diameter	52 mm
d - inner diameter	25 mm
B - thickness	15 mm
D_b - ball diameter	7.2 mm
N_b - number of balls	24 balls

The FFT spectrum was divided into a number of six bands, each band is specific of some causes leading to dynamic equipment failure. Thus, Band No. 2 is specific for the unbalances of the equipment, Band No. 3 for the misalignments, Band No. 4 for the clearances and looseness, Band No. 5 for the possible defects of rolling bearings, and Band No. 6 confirms the advanced condition of defects in rolling bearings by detecting the so-called "haystacks" [10].

The limits' calculation of these bands is done as follows:

1. Band No. 1: $0 \div 0.8 \times F_s$;
2. Band No. 2: $0.8 \times F_s \div 1.2 \times F_s$;
3. Band No. 3: $1.2 \times F_s \div 2.5 \times F_s$;
4. Band No. 4: $2.5 \times F_s \div 5.5 \times F_s$;
5. Band No. 5: $5.5 \times F_s \div 0.5 \times F_{max}$;
6. Band No. 6: $0.5 \times F_{max} \div F_{max}$.

where: F_{max} is the maximum frequency that is chosen depending on the type of equipment, the rotating speed and the type of used bearing. For this experiment will be F_{max} = 1000 Hz.

Thus, the limits' values of these bands calculated in this experiment will be:

1. Band No. 1: 0 ÷ 13.33 Hz;
2. Band No. 2: 13.33 ÷ 19.99 Hz;
3. Band No. 3: 19,99 ÷ 41.65 Hz;
4. Band No. 4: 41.65 ÷ 91.63 Hz;
5. Band No. 5: 91.63 ÷ 500 Hz;
6. Band No. 6: 500 ÷ 1000 Hz.

Based on expressions (1) ÷ (4) from first Section, the characteristic defect frequencies of this type of bearing have the following values: F_c = 6.81 Hz, F_{BPO} = 81.45 Hz, F_{BPI} = 118.55 Hz, F_{RE} = 43.39 Hz, F_{BPRE} = 86.78 Hz. Knowing that the rotating speed is 1000 rpm, the fundamental frequency will be: F_s = 16.67 Hz.

3. EXPERIMENTAL RESULTS AND INTERPRETATIONS

3.1. FFT and BCS spectrums analysis of the rolling bearing which worked with an artificial defect on the outer raceway under loading of 14 N

In FFT spectrum analysis for all measuring directions (Fig. 3) the harmonics of F_{BPO} frequency were detected. Also, the fundamental frequency (F_s) predominating in Band No. 2 and its harmonics in Bands No. 3 and 4 were observed. These observations give information regarding the existence of an unbalance which is developed by loading of 14 N. Because on the horizontal FFT spectrum the F_s and its harmonics are predominant, the harmonics amplitudes of F_{BPO} ($4 \times F_{BPO} \div 9 \times F_{BPO}$) are much lower compared to them, which makes it difficult to interpret the existence of a defect on the outer raceway. Better clarity of harmonics' amplitudes of F_{BPO} can be obtained only by using the *Zoom* function of XMS software. During the experiment (Fig. 4a and 4b) in this direction the harmonics' amplitudes of F_{BPO} haven't had significant increases.

In vertical direction the $3 \times F_s$ harmonic that predominates in the first measurement (Fig. 4c) and the F_s that predominates in the 6th measurement (Fig. 4d) were observed. Also, in FFT spectrums the harmonics of F_{BPO} ($3 \times F_{BPO} \div 9 \times F_{BPO}$) were observed, that are much clearer than those in the horizontal direction and also the appearance of the harmonic $3 \times F_{BPO}$. During the experiment in this direction the harmonics' amplitudes of F_{BPO} haven't had significant increases.

In axial direction the $3 \times F_s$ harmonic that predominates in spectrums (Fig. 4e and 4f) were observed as well as the harmonics' amplitudes of F_{BPO} ($3 \times F_{BPO} \div 12 \times F_{BPO}$) that are much clearer. During the experiment in this direction the harmonics' amplitudes of F_{BPO} haven't had significant increases.

In BCS spectrums analysis for all measuring directions, the F_{BPO} frequency and its harmonics, with much clearer amplitudes than the FFT spectrums, were detected. Also, the $1 \times F_s$ (*-1* and *1*) and $2 \times F_s$ (*-2* and *2*) sidebands, which confirm the existence an unbalance developed by loading of 14 N, were detected. In horizontal and vertical directions during the experiment the amplitudes of F_{BPO} and its harmonics were more obvious than those in the axial direction (in horizontal and vertical directions the highest values occurring in the 4th measurement and in axial direction in the 6th measurement) as can be observed in Fig. 5.

Although the amplitudes of F_{BPO} and its harmonics increased during the experiment in all directions of the measurement, when the rolling bearing was dismounted (Fig. 6) it didn't have any damage caused by the implementation of the defect on the outer raceway.

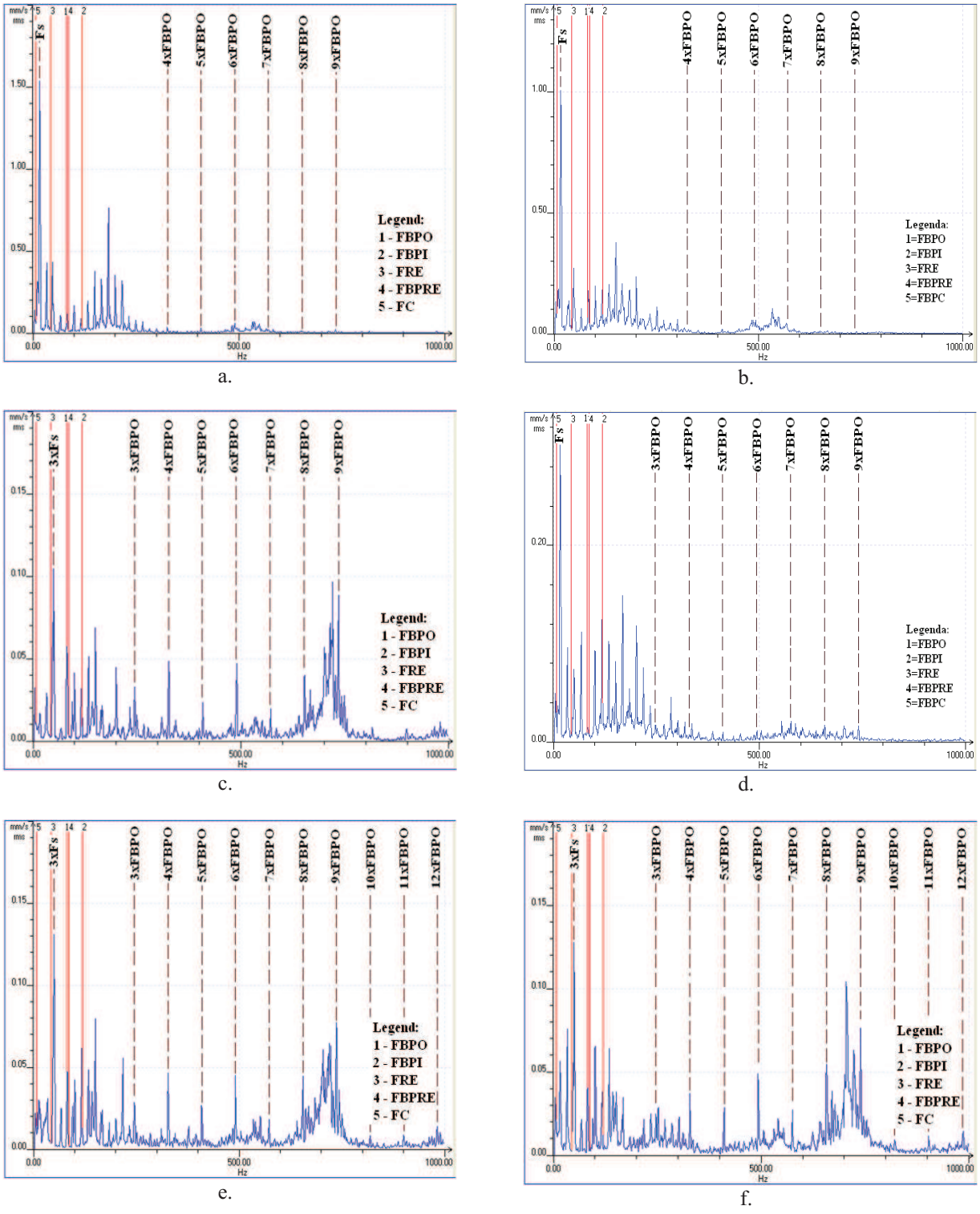

Fig. 4. FFT spectrums of bearing operating under loading of 14 N: a. - in horizontal direction for the 1st measurement; b. - in horizontal direction for the 6th measurement; c. – in vertical direction for the 1st measurement; d. – in vertical direction for the 6th measurement; e. -in axial direction for the 1st measurement; f. - in axial direction for the 6th measurement

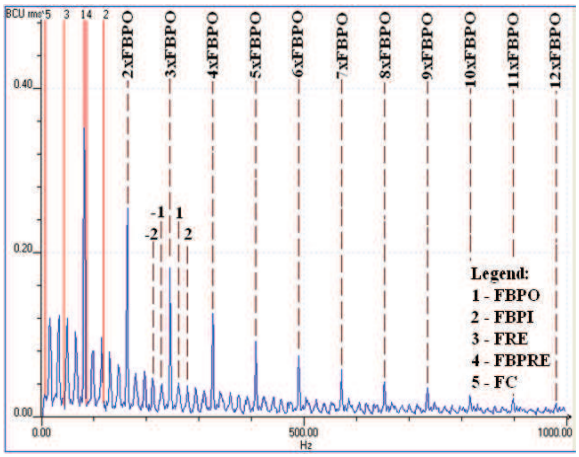

a.

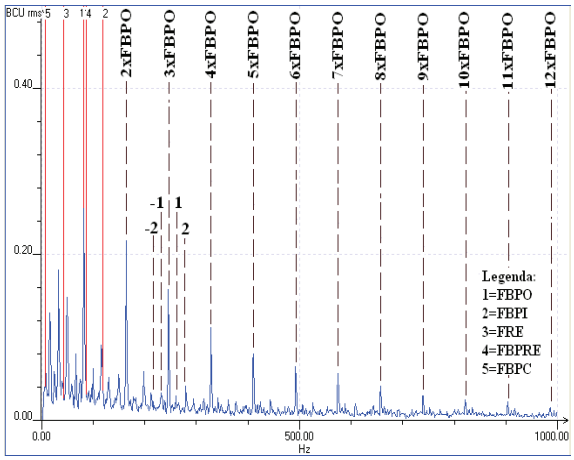

b.

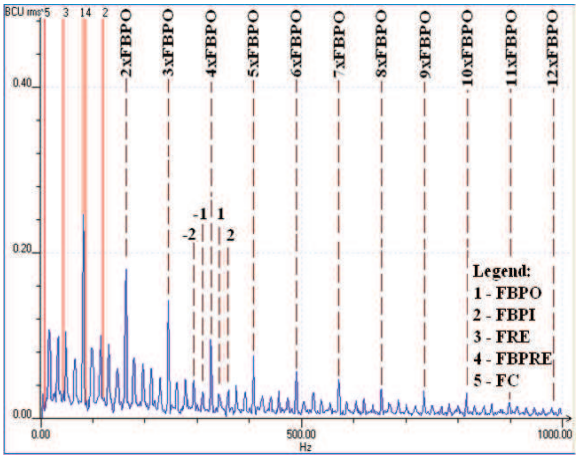

c.

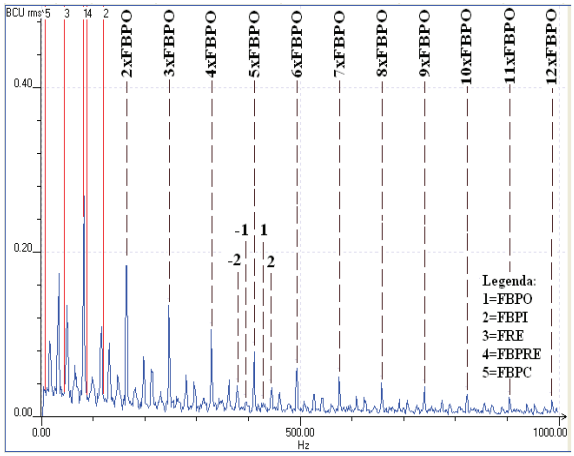

d.

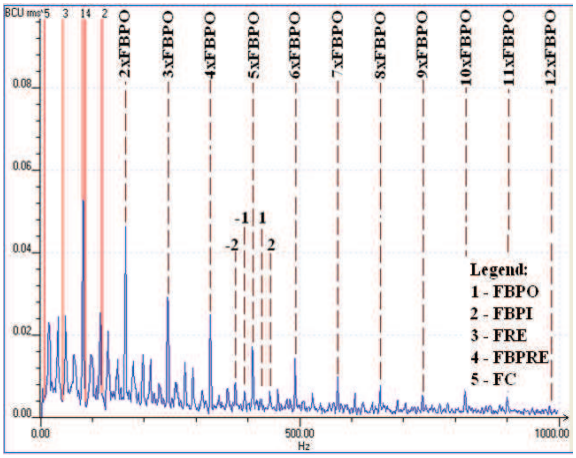

e.

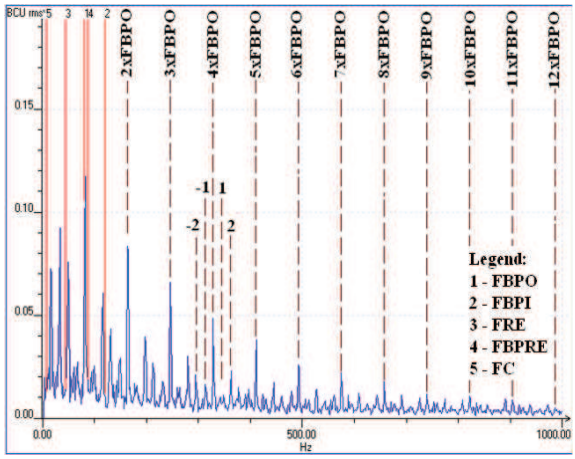

f.

Fig. 5. BCS spectrums of bearing operating under loading of 14 N: a. - in horizontal direction for the 1st measurement; b. - in horizontal direction for the 6th measurement; c. - in vertical direction for the 1st measurement; d. - in vertical direction for the 6th measurement; e. - in axial direction for the 1st measurement; f. - in axial direction for the 6th measurement

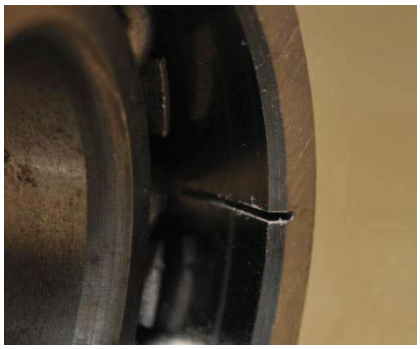

Fig.6. Evolution of rolling bearing degradation with artificial defect on the outer raceway after its operation under loading of 14 N

3.2. FFT and BCS spectrums analysis of the rolling bearings which worked with an artificial defect on the outer raceway under loading of 28 N

During this experiment in FFT spectrums it was observed that by increasing of loading the harmonics' amplitudes of F_{PBO} increased and the *1x* F_c (*-1'*and *1'*) sidebands appeared. Also, it was observed that the F_s frequency and its harmonics predominate in spectrums. In horizontal direction (Fig. 7), the number of harmonics of F_{PBO} increased from $4 \times F_{PBO} \div 9 \times F_{PBO}$ to $3 \times F_{PBO} \div 12 \times F_{PBO}$ and their amplitudes are much clearer. In vertical direction (Fig. 8) the number of harmonics of F_{PBO} increased from $3 \times F_{PBO} \div 9 \times F_{PBO}$ to $3 \times F_{PBO} \div 12 \times F_{PBO}$.

In axial direction (Fig. 9) it was observed that by increasing of loading the $8 \times F_{PBO}$ and $9 \times F_{PBO}$ harmonics have high amplitudes (even higher than the F_s frequency and its harmonics). The increases of F_{PBO} amplitudes during the experiment can confirm the existence of rolling bearing damage due to implemented defect on the outer raceway.

During this experiment in BCS spectrums analysis (Fig. 10, 11 and 12) for all measuring directions it was observed that by increasing the loading, the amplitudes of F_{PBO} and of its harmonics increased. Also, the $1 \times F_s$ (*-1* and *1*), $2 \times F_s$ (*-2* and *2*) and $1 \times F_c$ (*-1'* and *1'*) sidebands were observed.

These amplitudes increases of the harmonics of F_{PBO} from FFT spectrums and of the F_{PBO} frequency and of its harmonics from BCS spectrums, as well as the appearance mode of the sidebands give the evolution mode of the artificial defect on the outer raceway when loading is increased from 14 N to 28 N. At the dismounting of the rolling bearing (Fig. 13) these observations are confirmed by establishing the evolution mode of the artificial defect on the outer raceway (a groove of about 8 mm, along the outer raceway in area of the artificial defect and a thermal wear on the balls from the row that is it in contact with the artificial defect were developed). Thermal wear in this bearing is present by a color changing (a blackening) of the superficial layer of the balls' material.

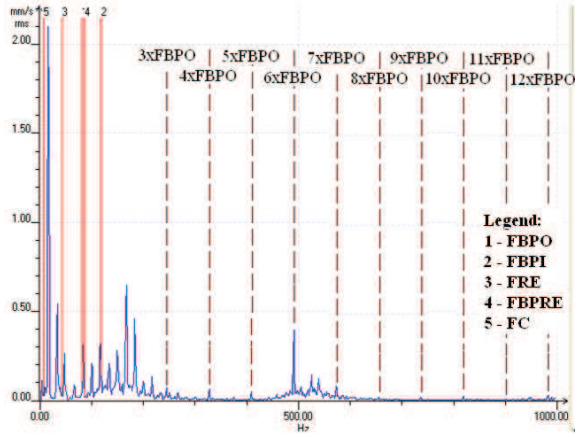

Fig. 7. FFT spectrum of bearing operating under loading of 28 N in the horizontal direction for the 5th measurement

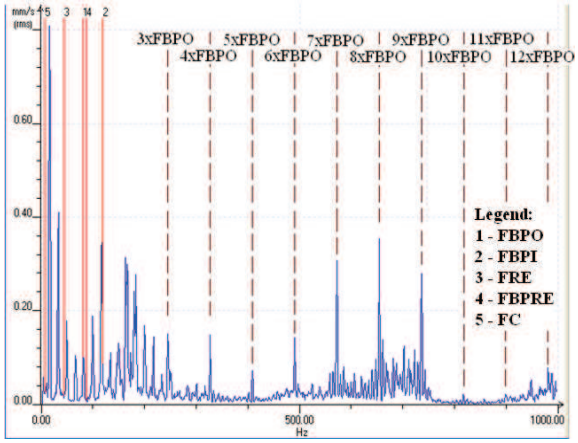

Fig. 8. FFT spectrum of bearing operating under loading of 28 N in the vertical direction for the 3rd measurement

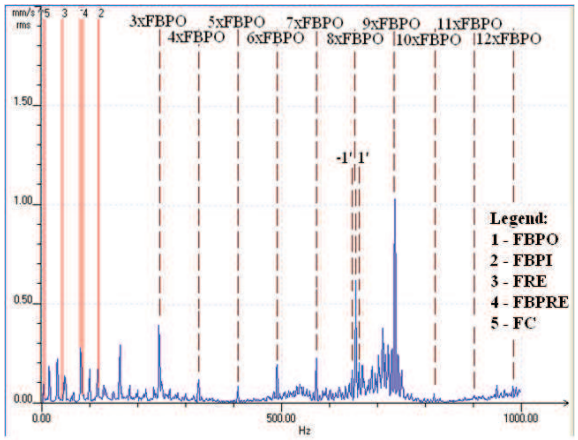

Fig. 9. FFT spectrum of bearing operating under loading of 28 N in the axial direction for the 3rd measurement

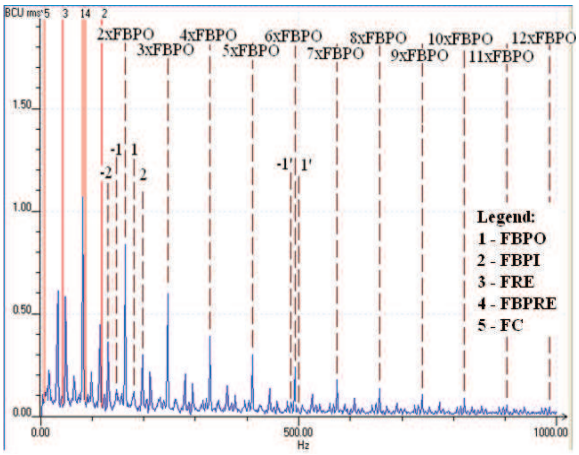

Fig. 10. BCS spectrum of bearing operating under loading of 28 N in the horizontal direction for the 6th measurement

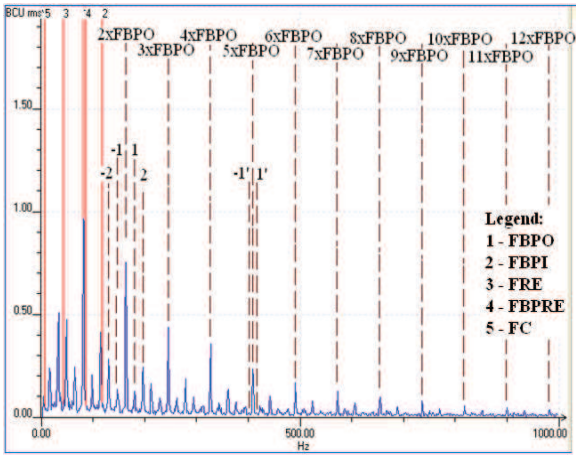

Fig. 11. BCS spectrum of bearing operating under loading of 28 N in the vertical direction for the 5th measurement

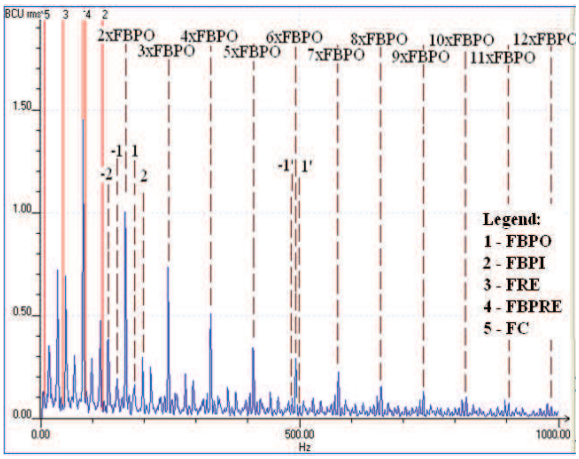

Fig. 12. BCS spectrum of bearing operating under loading of 28 N in the axial direction for the 6th measurement

Fig. 13. Evolution of rolling bearing degradation with artificial defect on the outer raceway after its operation under loading of 28 N

3.3. FFT and BCS spectrums analysis of the rolling bearings which worked with an artificial defect on the outer raceway under loading of 42 N

In FFT spectrums it was observed that by increasing of loading, the harmonics' amplitudes of F_{PBO} and the *1x* F_c (*-1'* and *1'*) sidebands are much clearer in all measuring directions. Also, the F_s frequency and its harmonics that predominate in spectrums, were observed. In horizontal direction (Fig.14) at the 6th measurement the harmonics' amplitudes of F_{BPRE} were observed, which confirms the damage of the rolling bearing's ball. In vertical and axial directions this defect characteristic frequency was observed even from the 5th measurement as can be seen in Fig. 15 and 16.

In BCS spectrums for all measuring directions was observed that by increasing of loading, the amplitudes of F_{BPO} and of its harmonics increased.

Thus, in horizontal and vertical directions these amplitudes increased until the 4th measurement, then at the 5th measurement the amplitudes of F_{BPRE} and F_{RE} frequencies were observed. At the 6th measurement, the amplitudes of F_{BPRE} and F_{RE} frequencies and of its harmonics are much higher than F_{BPO} frequency and its harmonics that are more difficult to observe. In axial direction the amplitudes of F_{BPO} and of its harmonics are difficult to observe even from the 5th measurement. These higher amplitudes of F_{BPRE} and F_{RE} frequencies suggest that the balls' damage is more extensive than the outer raceway damage. These observations were confirmed at the dismounting of the rolling bearing (Fig. 20). Thus, along the outer raceway the groove expanded from 8 mm to 41 mm (Fig. 20b), in addition to the thermal wear of the balls there was also a removal of material from the surface layer (Fig. 20a) and inner raceway has a thermal wear with small dimples (small removal of material - fig. 20c).

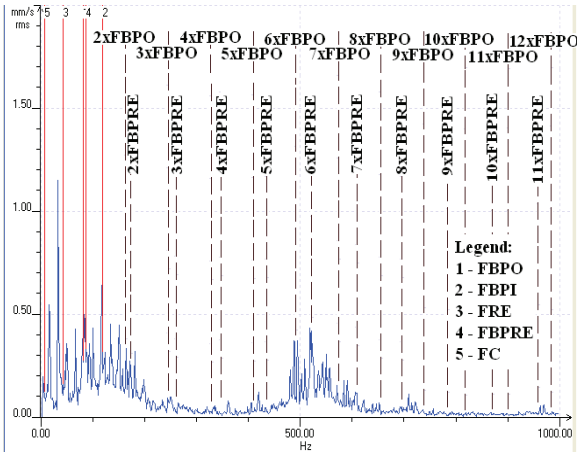

Fig. 14. FFT spectrum of bearing operating under loading of 42 N in the horizontal direction for the 6th measurement

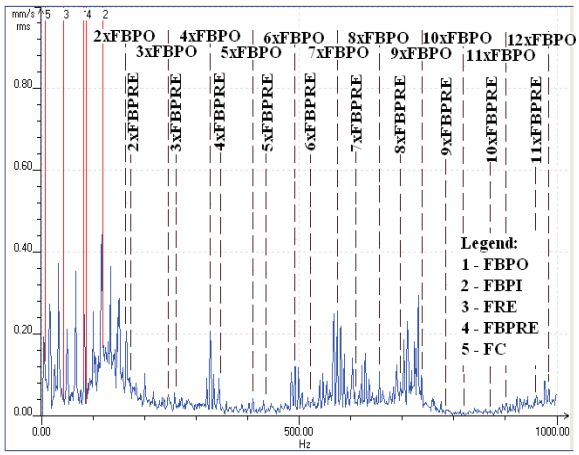

Fig. 15. FFT spectrum of bearing operating under loading of 42 N in the vertical direction for the 5th measurement

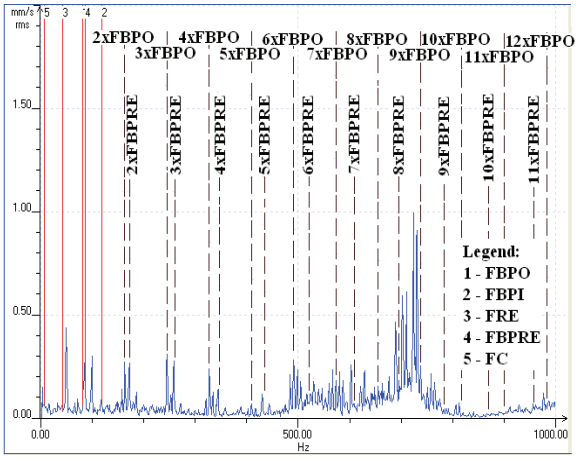

Fig. 16. FFT spectrum of bearing operating under loading of 42 N in the axial direction for the 5th measurement

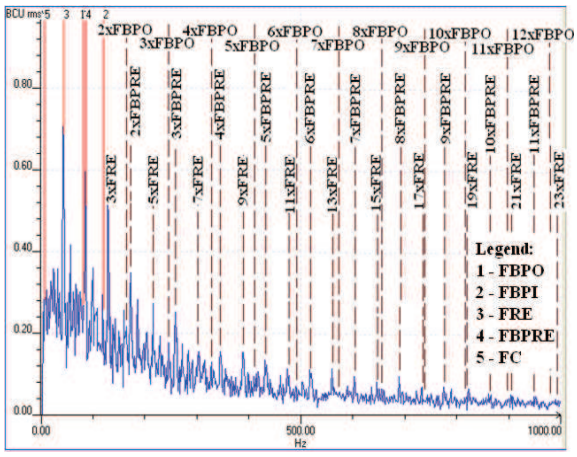

Fig. 17. BCS spectrum of bearing operating under loading of 42 N in the horizontal direction for the 5th measurement

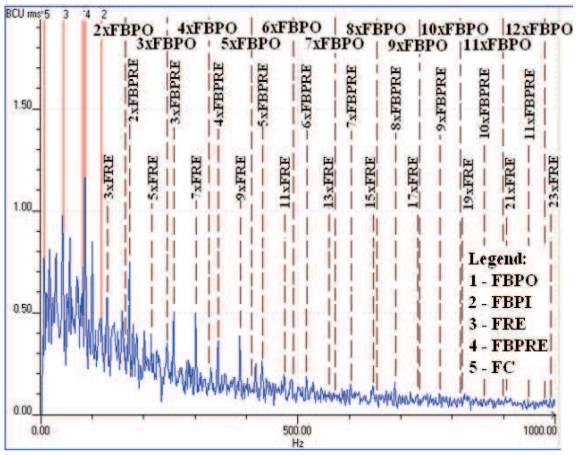

Fig. 18. BCS spectrum of bearing operating under loading of 42 N in the vertical direction for the 5th measurement

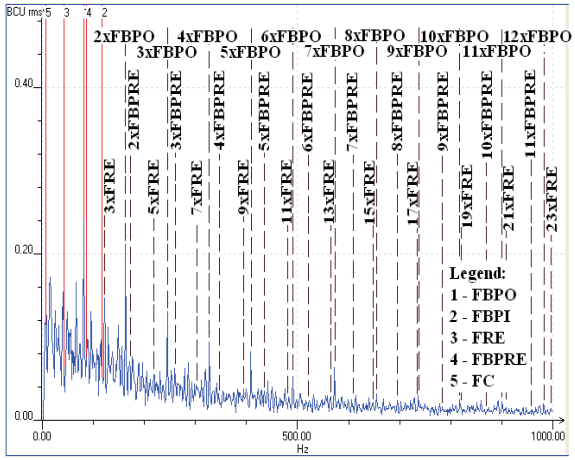

Fig. 19. BCS spectrum of bearing operating under loading of 42 N in the axial direction for the 4th measurement

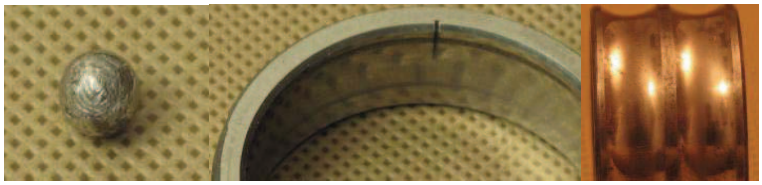

a. b. c.

Fig. 20. Evolution of rolling bearing degradation with artificial defect on the outer raceway after its operation under loading of 42 N: a. – on ball; b. – on outer raceway; c. – on inner raceway

4. CONCLUSIONS

Measurement and analysis of vibrations, over time, in different points of dynamic equipments' rolling bearings represent a safe and effective measure for the diagnosis and prediction of their technical state as well as of the entire equipment. The FFT and BCS spectrums analysis give the most effective information on the causes of rolling bearings deterioration during the time passing, but they also give prediction on their remaining lifetime. Thus, the FFT spectrums of this experimental research give information by the appearance of rotation speed amplitudes, F_s, and its harmonics on the existence of an unbalance created by the used loadings, and by the appearance of characteristic defect frequencies' harmonics (F_{BPO}, F_{BPRE} and F_{RE}) on the presence of defects from rolling bearing components. These harmonics of characteristic defect frequencies have random variations in their amplitude both in time and spectrum width. These random variations don't provide sufficient information regarding the evolution mode of rolling bearing deterioration both due to unbalance and when faults occur in their components. On the other hand, in BCS spectrums, amplitudes of characteristic defect frequencies and of its harmonics decrease asymptotically from characteristic defect frequencies to the last harmonic. The BCS spectrums give information regarding the existence of unbalance by the appearance of $1x\ F_s$ and $2x\ F_s$ sidebands of characteristic defect frequencies, as well as the existence of different diameters of the rolling elements by $1x\ F_c$ and $2x\ F_c$ sidebands. Also, by the appearance and evolution mode of characteristic defect frequencies amplitudes and of its harmonics, BCS spectrums give beneficial information regarding the evolution mode of bearing degradation during the time passing. Thus, in order to have efficiency of the diagnosis and of the prediction of rolling bearings, it is necessary to use FFT and BCS spectrums analysis. For detecting of characteristic defect frequencies, the knowledge of rolling bearing geometrical characteristics is also necessary, but in order to have an effective diagnosis and prediction, it is required to have an experienced and responsible staff.

REFERENCES

[1] Orhan S., Akturk N., Celik V.: *Vibration monitoring for defect diagnosis of rolling element bearings as a predictive maintenance tool: Comprehensive case studies*, NDT&E International, 2006, Vol. 39, No. 4, pp. 293 – 298.

[2] Băjenaru S., Ganga M., Valentin V., Danciu A.: *The study of the diagnosis theory applied for predictive maintenance*, Research Journal of Agricultural Science, 2009, Vol. 41, No. 2, pp. 338-350.

[3] Balerston H. L.: *The Detection of Incipient Failure in Bearings*, Materials Evaluation, 1996, Vol. 27, pp. 121 – 128.

[4] Tse P., Peng Y., Yam R.: *Wavelet analysis and envelope detection for rolling element bearing fault diagnosis their effectiveness and flexibilities,* Journal of Vibration and Acoustics, 2001, Vol. 123, pp. 303–310.

[5] Mobley K. R.: *Root Cause Failure Analysis*, Reed Elsevier, USA, 1999.

[6] Nadabaica D. C., Bibire L., Andrioai G.: *Study of the advantages of predictive maintenance in the monitoring of rolling bearings,* Environmental Engineering and Management Journal, 2012, Vol. 11, No. 12, pp 2233-2238.

[7] Ragulskis K., Yurkauskas A.: *Vibration of Bearing*, Hemisphere Publishing Corporation, Bristol, 1989.

[8] Rieger N. F., Crofoot J. F.: *Vibration of Rotationary Machinary,* Rochester Institute of Tehnology, 1977, pp.69-77.

[9] Al-Hazmi M.W.: *The Effect Of The Manufacturing Errors On The Dynamic Performance Of Gears,* Journal of Engineering & Architecture, 2011, Vol. 4, No. 2, pp. 37-53.

[10] Dennis H. S.: *Signal Processing For Effective Vibration Analysis*, IRD Mechanalysis, Inc. Columbus, Ohio, 1995.

Dumitru - Cristinel NADABAICA is PhD student and associate assistant in Environmental Engi-neering and Mechanical Engineering Department, Engineering Faculty, "Vasile Alecsandri" University of Bacau. In his works he explores issues of the diagnostic of process equipments failure and the prognosis of their remaining lifetime.

Prof. **Valentin NEDEFF**, PhD is Rector of "Vasile Alecsandri" University of Bacau and professor in Environmental Engi-neering and Mechanical Engineering Department, Engineering Faculty. In his scientific work he deals with research in mechanical and environmental field.

Prof. Stanisław RADKOWSKI, professor in the Institute of Vehicles of the Warsaw University of Technology. In his scientific work he deals with vibroacoustic diagnosis, technical risk analysis and energy harvesting.

Dr inż. Jędrzej MĄCZAK, PhD, is an assistant professor at the Institute of Vehicles of the Warsaw University of Technology. His scientific interests are distributed diagnostic systems, machine diagnostics and analysis of the vibroacoustic signals.